Available on the CMS information server CMS AN 09-xxx

CMS Analysis Note

The content of this note is intended for CMS internal use and distribution only

September 3, 2009

Magnetic Field Studies in the CMS Muon Endcap

Didar Dobur[1] and Michael Schmitt[2]

[1] University of Florida, Gainesville, Florida, USA
[2] Northwestern University, Evanston, Illinois, USA

Abstract

The magnetic field map in the muon endcap region has been verified using cosmic ray data taken in Fall 2008 (CRAFT). The method compares the observed deflection of muons in YE1 and YE2, as measured using segments in the CSCs, to the predicted deflection based on extrapolations of tracker tracks. The data indicate that the old magnetic field map represented a magnetic field that is too high by 6% in YE1, and too low by 2% in YE2.

1 Introduction

In Winter 2009, the observed deflection of muons in the muon barrel detector were not reproduced accurately by the simulation. After much effort, it was shown that improvements to the magnetic field map were needed, traced back to the way TOSCA implements magnetic field boundary conditions at infinity. Naturally, the question arose as to the agreement of the improved magnetic field map with the data in the endcaps. This note documents the result of a study based on CRAFT data, meant to answer that question.

2 Method

A cross-sectional view of the CMS detector showing the CSC's is given in Fig. 1. One notes that the chambers in ME1/2 and ME1/3 on one side, and ME2/2 on the other, bracket the return yoke disk YE1. The magnetic field is concentrated in the iron of the yokes YE1, YE2 and YE3. To a significant degree, the path of the muon through ME1, YE1 and ME2 amounts to a simple deflection in a dipole field. The angle of between the straight-line segments in ME1 and ME2 is directly related to the magnetic field strength in YE1, as well as the path length projected into the plane perpendicular to $\vec{B}$. This angle is easily inferred from the reconstructed segments in the ME1 and ME2.

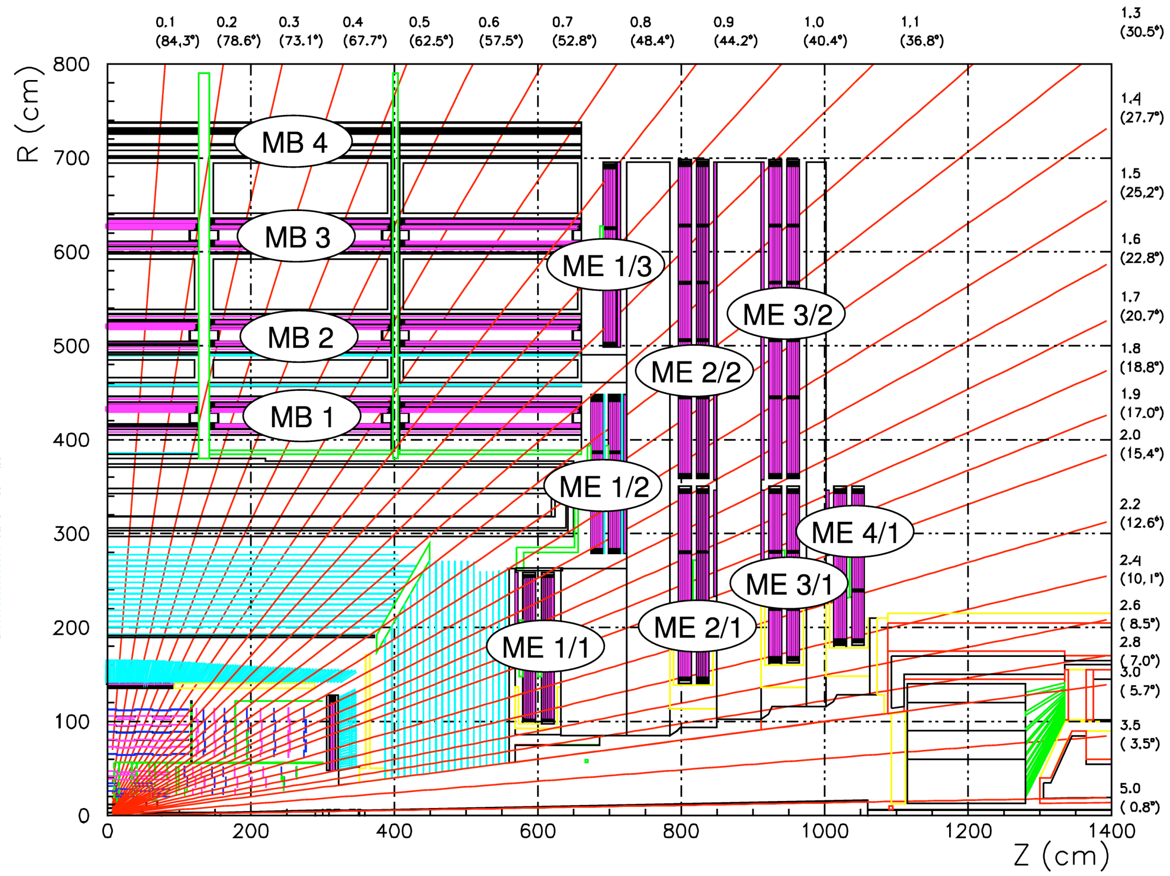

Figure 1: A cross-sectional view of the CMS detector.

2.1 Event Sample

Muons from cosmic rays come in a wide range of momenta and angles. Even selecting those which follow a useful trajectory, the momentum is *a priori* completely uncertain. We must know the momentum of each muon in order to compute the expected deflection through YE1. We use tracks reconstructed in the silicon tracker, whose momentum scale is correct by definition. Thus we compare the deflection measured with CSC's segments to a prediction obtained by extrapolating tracker tracks through the magnetic field in the endcap yokes into the CSC's.

Of the 300M muon-triggered events recorded in CRAFT, only a minute portion are useful for this study. We developed an effective filter to select events based on relatively simple criteria which nonetheless gave us an excellent sample of events for this study. The filter passes events which have a good global muon and/or both a good tracker track and a good stand-alone muon. The definition of "good" is as follows:

- "good" global muon:
    1. $p > 3$ GeV/c
    2. at least 8 hits in the tracker
    3. at least 9 CSC hits
    4. $\chi^2/\mathrm{NDF} < 20$
- "good" stand-alone muon:
    1. $p > 3$ GeV/c
    2. at least 9 CSC hits
    3. $Z_{\mathrm{length}} > 200$ cm
- "good" tracker track:
    1. $p > 3$ GeV/c
    2. at least 8 hits in the tracker

Here, Z_{length} is the difference between the largest and the smallest Z coordinate for hits on the track. The cuts on Z_{length} ensure that the tracks are long enough to pass through at least one iron yoke, thereby giving a momentum measurement. Overall, these cuts are quite loose. This filter is implemented in the `CSCSkim` offline analysis code, which contains a number of CSC-based filters. This so-called *BFieldStudies* skim is type 9 in `CSCSkim`. A typical event is displayed in Fig. 2.

Only 119,743 events are selected from the roughly 300M muon-triggered events recorded in CRAFT. They are used for the studies of the magnetic field in the endcaps reported in this note, as well as for large-scale alignment of the endcaps and studies of stand-alone muons.

2.2 Energy Loss

The cosmic ray muons in our sample generally enter in the upper half of the detector ($y > 0$) and exit in the lower half ($y < 0$). Consequently, the difference in energies in the endcaps and in the tracker has opposite sign for the upper and lower halves. This energy loss is not small – in YE1 alone, for example, a muon loses typically 1.4 GeV.

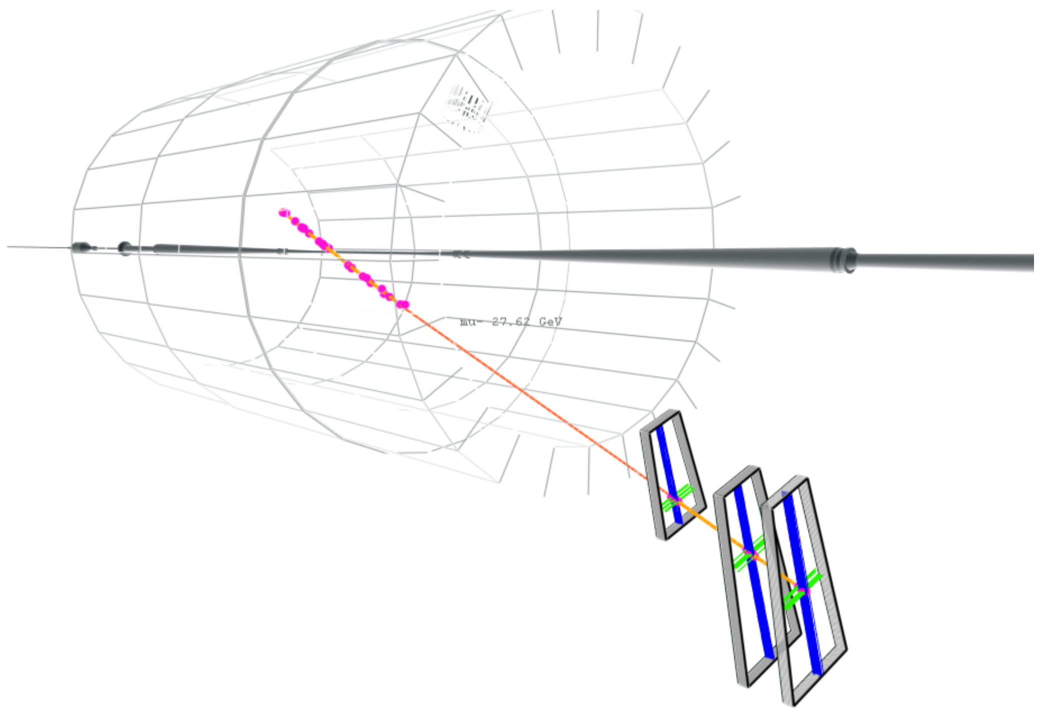

Figure 2: A typical event selected by `CSCSkim`, type 9.

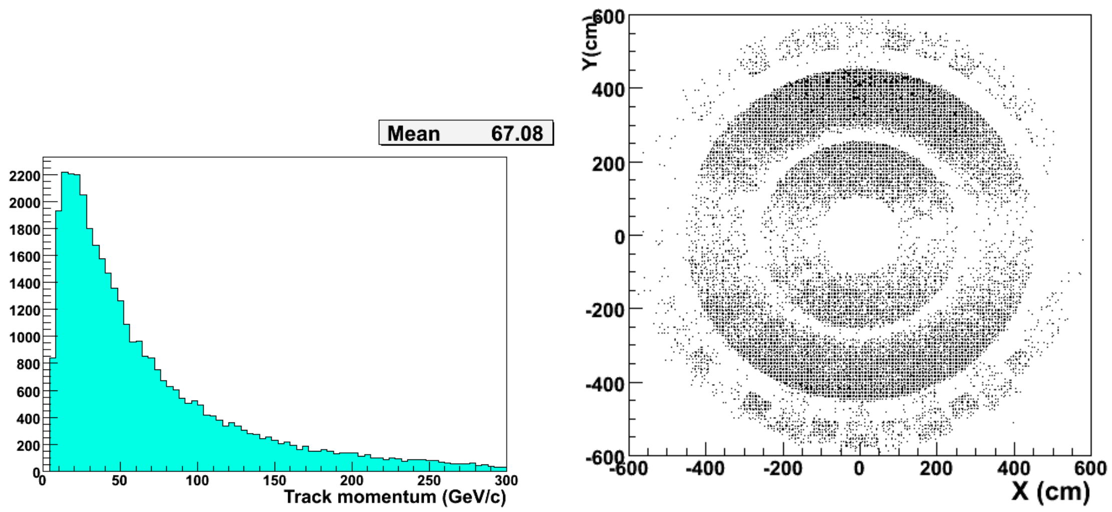

Figure 3: Basic distributions of momentum measured in the tracker (left), and the (X, Y) coordinates in ME$\pm$1/1 for the stand-alone muons. The three rings in ME$\pm$1/1 are easily discerned.

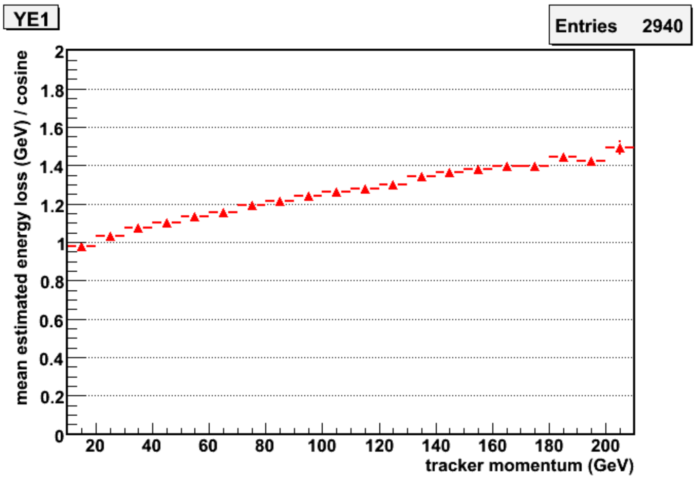

Figure 4: Mean normalized energy loss, $\langle \Delta \tilde{p} \rangle$, as a function of tracker momentum.

We made a simple check of the energy loss as assumed in the propagation of tracker tracks to ME2. The propagator returns the momentum vector, so we can easily obtain the energy difference $\Delta p = p_{ME3} - p_{ME2}$ as well as the inclination of the track through YE1, characterized by $\cos \alpha$ where α is the angle with respect to the normal of YE1 (i.e., the z-axis). For each event, we computed the normalized energy loss, $\Delta \tilde{p} = \Delta p / (L \cos \alpha)$, where $L \approx 34 X_0$ is the thickness of YE1 in radiation lengths. Fig. 4 shows the mean $\langle \Delta \tilde{p} \rangle$ as a function of p_{ME2}. The classic logarithmic rise is evident, and can be directly compared with the known energy loss of charged particles in iron [2]. The agreement is good at the percent level, indicating there is no major problem with this aspect of the energy loss as included in the propagation of tracker tracks. One should realize that this is not a *measurement* of the energy loss – only a cross-check that the propagation is done in a consistent manner.

2.3 Muon Deflection

The basic assumption is that the bending occurs only inside the iron yokes, and that the direction of the magnetic field is in the $\hat{s}$ direction, where the unit vector $\hat{s}$ points away from the z-axis in cylindrical coordinates. The segments reconstructed in ME1 and ME2 provide global coordinates and directions. The direction vectors can be normalized to unit length, call them $\hat{u}_1$ and $\hat{u}_2$ for ME1 and ME2. A simple measure of the deflection of the muon by the magnetic field is

$$\delta \equiv \sin \epsilon = (\hat{u}_1 \times \hat{s}) \cdot \hat{u}_2. \quad (1)$$

An elementary calculation relates ϵ to the magnetic field and the component of the momentum perpendicular to the field, $p_\perp$,

$$\tan(2\epsilon) = 0.3 BL \left(\frac{q}{p_\perp} \right) \quad (2)$$

where L is the thickness of the iron yoke in the z direction. For small ϵ, we have $\tan(2\epsilon) \approx 2\delta(1 - \frac{3}{2}\delta^2)$, which is quite accurate for $\epsilon < 0.35$. Crudely speaking, $\delta \propto B$.

We will measure δ from the CSC's and compare to a "predicted" value from extrapolating the tracker track to ME1, through YE1, and to ME2. The predicted deflection δ_{pred} is determined by the magnetic field map, while the measured deflection δ_{meas} depends on the real magnetic field. If $\delta_{\text{meas}} < \delta_{\text{pred}}$, then the magnetic field in the map is too high, since $\delta_{\text{meas}}/\delta_{\text{pred}} = B_{\text{true}}/B_{\text{map}}$. As we will see below, $\delta_{\text{meas}}/\delta_{\text{pred}} \approx 0.95$.

This method retains some advantages worth noting. First, it demands from the CSC's only the measurement of directions of straight line portions of tracks, which is well within their capability. Comparisons of the momentum measured in the muon system and in the tracker suffer from a lack of good alignment information for the CSC's – basically they cannot measure momentum accurately, for the CRAFT data. Similarly, a comparison of the projected arrival of the muon in a chamber to the measured arrival suffers if the chamber alignment is unknown (though a careful handling of positive and negative muons might solve this problem). Finally, this method is data-driven, with no need for input from the simulation. In fact, a simulated cosmic ray sample can be used for verifying the method, by checking that $\delta_{\text{meas}} = \delta_{\text{pred}}$ within statistical errors. One of the analyses of the barrel muon drift tubes used essentially this same method [3].

The quality of the measurement of δ restricts the useful range of $p_\perp$ from 5 to 30 GeV. Multiple scattering for low momenta and resolution on the directions of the CSC segments limit the low and high range of momentum, respectively.

Plots of δ_{meas} and δ_{pred} for narrow ranges of $p_\perp$ are shown in Fig. 5. The distributions are also reasonably narrow and symmetric, justifying the use of a profile plot to study δ as a function of $p_\perp$. Fig.6 shows $\langle\delta\rangle$ as a function of $p_\perp$, for positive and negative muons separately. The triangles represent δ_{meas} while the crosses represent δ_{pred} – they are quite close to each other for the range $0.03 < 1/p_\perp < 0.2$. It makes sense to look at the ratio $\delta_{\text{meas}}/\delta_{\text{pred}}$, which is shown in Fig. 7, for the restricted range $0.03 < 1/p_\perp < 0.2$. A clean, symmetric peak is observed. A Gaussian fit to the central core gives

$$\frac{\delta_{\text{meas}}}{\delta_{\text{pred}}} = 0.942 \pm 0.008 \qquad \text{(YE1)} \tag{3}$$

which is surprisingly precise. We checked for non-linear effects by plotting this ratio as a function of $1/p_\perp$ – see Fig. 8, which shows the mean $\langle\delta_{\text{meas}}/\delta_{\text{pred}}\rangle$ from a profile histogram, as well as the peak position of Gaussian functions fit in narrow slices of $1/p_\perp$. The value in Eq. 3 is constant and there is no sign of any non-linearity.

In order to verify that the significant deviation from one (Eq. 3) is not due to some aspect of the analysis method, we performed the analysis on simulated cosmic ray events. The distribution of $\delta_{\text{meas}}/\delta_{\text{pred}}$ is very similar to Fig. 7, except that the peak is centered on one. A fit to the peak gave $(\delta_{\text{meas}}/\delta_{\text{pred}})_{\text{MC}} = 1.03 \pm 0.02$. A direct overlay of the distributions from real and simulated events is shown in Fig. 9, which shows that the simulation matches the real data well, *except* for the position of the peak, which is clearly displaced.

We compared $\langle\delta_{\text{meas}}/\delta_{\text{pred}}\rangle$ measured in the two endcaps. As seen in Fig. 9, there is no difference. We also checked the stability of the ratio with ϕ and also radius from the beam, and found no statistically significant deviations.

The result for YE1 seem stable and robust, so we extend the method to YE2, which is bracketed by ME2 and ME3. The same procedure described above was followed, with similar results. The main difference with respect to the YE1 study is that the distributions of both δ_{meas} and δ_{pred} are somewhat broader, due to the multiple scattering in YE1 and the longer extrapolation distance for the tracker tracks.

It is worth noting that the magnetic field in YE2 is roughly 30% weaker than in YE1, accord-

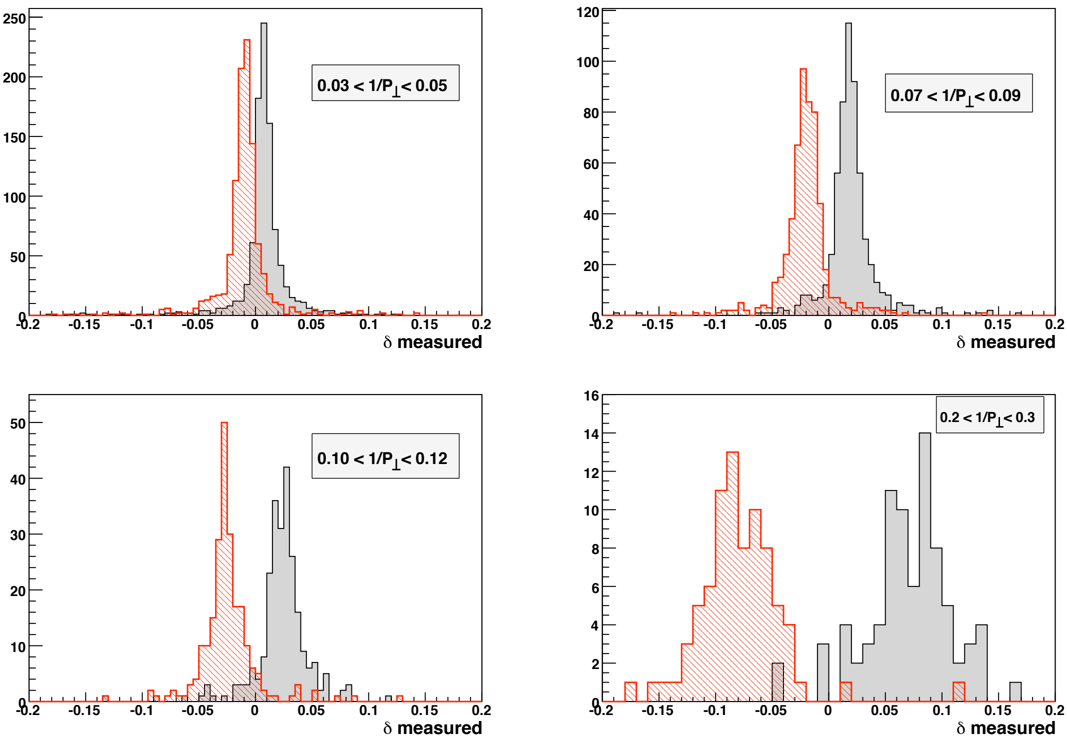

Figure 5: Deflections δ_{meas} for narrow ranges of $p_\perp$, separating positive and negative muons. The distributions for δ_{pred} are narrower.

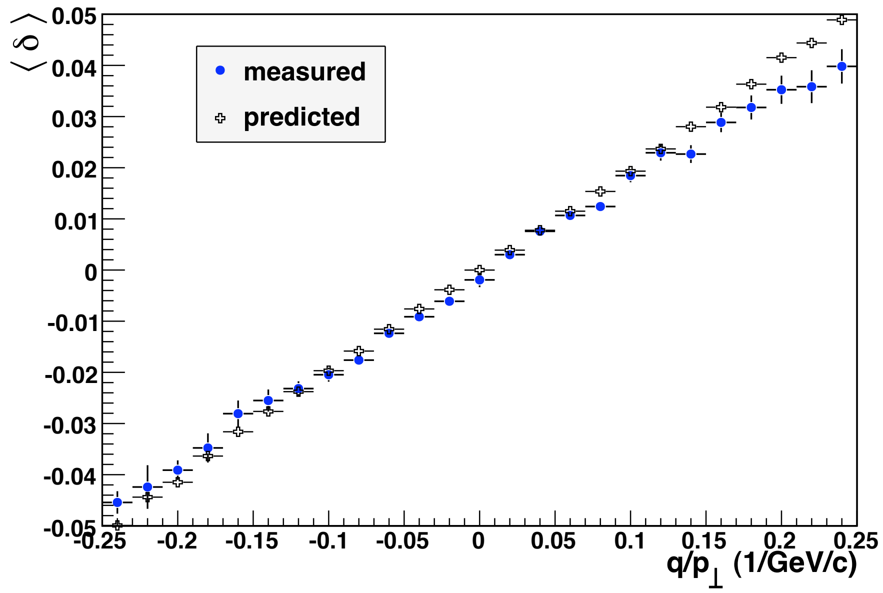

Figure 6: Mean deflections $\langle\delta\rangle$ as a function of $q/p_\perp$.

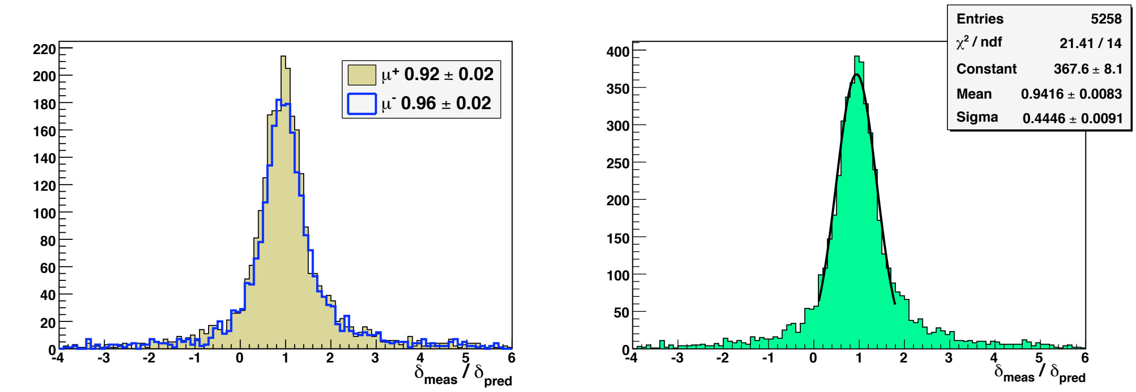

Figure 7: Distribution of the ratio $\delta_{\text{meas}}/\delta_{\text{pred}}$ for $0.03 < 1/p_{\perp} < 0.2$. The left plot shows positive and negative muons separately. They are combined in the right plot for fitting the central core to a Gaussian function.

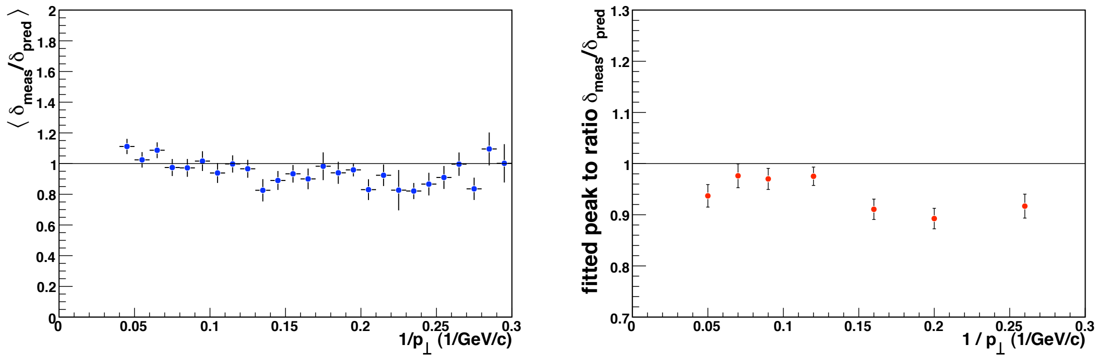

Figure 8: Mean ratio $\langle \delta_{\text{meas}}/\delta_{\text{pred}} \rangle$ as a function of $1/p_{\perp}$.

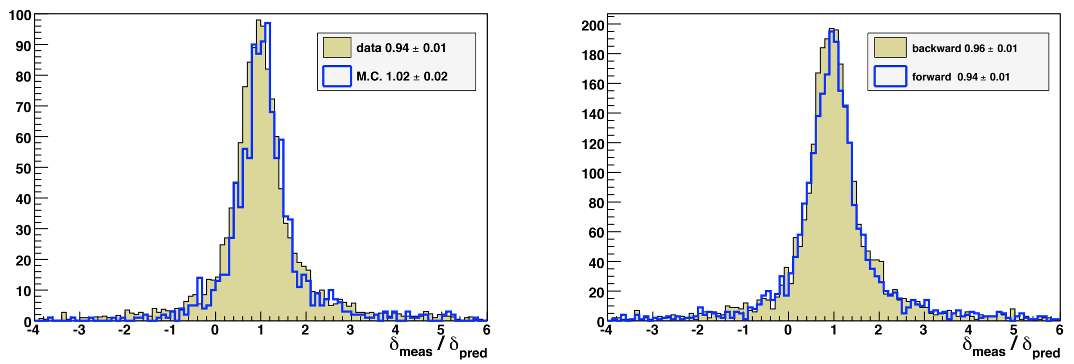

Figure 9: Comparisons of the distributions of the ratio $\delta_{\text{meas}}/\delta_{\text{pred}}$. On the left, real and simulated events. On the right, the two endcaps.

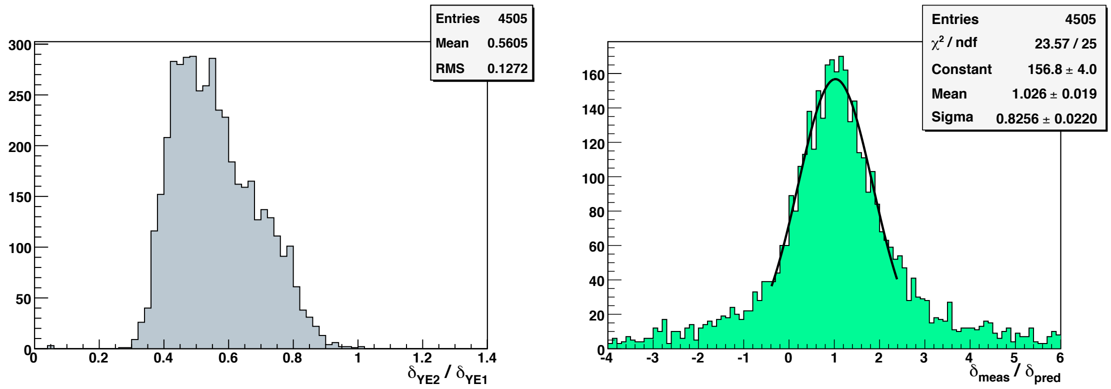

Figure 10: Results for YE2. On the left, the distribution of the ratio of δ_{pred} for YE2 relative to δ_{pred} for YE1, muon-by-muon. On the right, the ratio $\delta_{\text{meas}}/\delta_{\text{pred}}$.

ing to the magnetic field map. Fig. 10 confirms that for the same muon, δ_{pred} is smaller in YE2 than in YE1.

The distribution of the ratio $\delta_{\text{meas}}/\delta_{\text{pred}}$ computed for ME3 and ME (i.e., for YE2) is shown in Fig. 10. The main feature is a symmetrical Gaussian peak at the core of the distribution, with long tails. We fit the central core to a single Gaussian function and obtained

$$\frac{\delta_{\text{meas}}}{\delta_{\text{pred}}} = 1.026 \pm 0.019 \qquad (\text{YE2}) \tag{4}$$

which favors a value slightly larger than one, but is statistically consist with one at the percent level.

3 Discussion

The original magnetic field map, upon which the above measurements are based, was shown to suffer from a problem with the boundary conditions in TOSCA. An improved version of the map, validated in the barrel in detail, indicates small, uniform changes in the magnetic field in YE1 and YE2, as shown in Fig. 11. The figures suggest changes of approximately +6% in YE1, and -2% in YE2. These are precisely the opposite of what is indicated by the measurements here, Eq. 3 and 4.

4 Conclusions

The CRAFT data sample from 2008 allowed a quantitative study of the deflection of muons in the endcaps. Comparisons of a predicted deflection based on the extrapolation of tracker tracks to the measured deflection coming from muon track segments measured in the CSCs show that the real magnetic field is about 6% weaker in YE1 than represented in the magnetic field map. The data do not indicate any error for YE2, at the 2% level.

Acknowledgments

We are grateful to the dedicated members of the *Magnetic Field Task Force*, especially Nicola Amapane, Sara Bolognesi, Vyacheslav Klyukhin, Vassili Maroussov and Martijn Mulders,

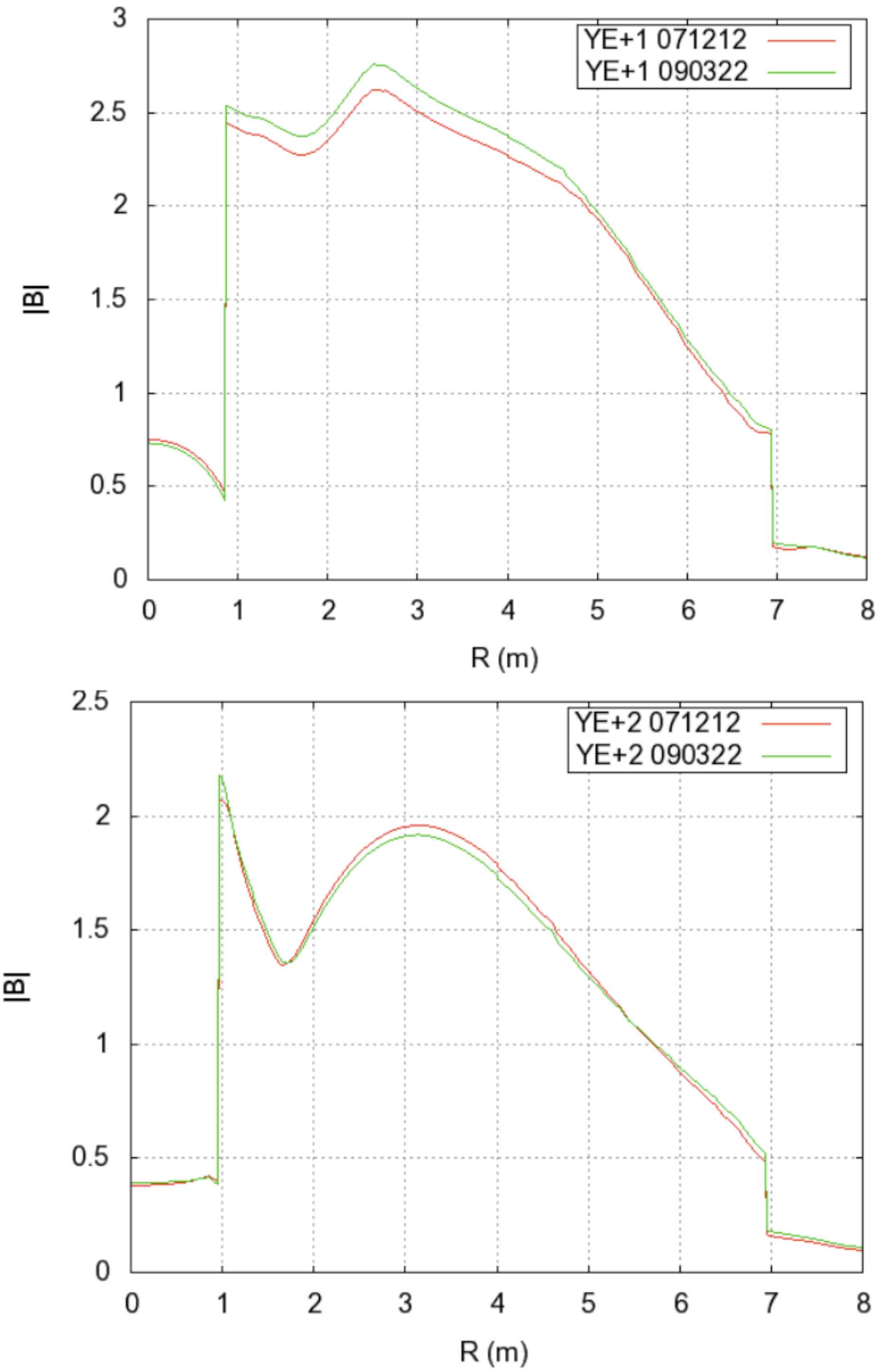

Figure 11: Traced of the magnitude of the magnetic field as a function of radius (from the beam line), inside YE1 (top plot) and YE2 (bottom plot). The key “071212” refers to the old map, and “090322” to the new.

who met many times over several months to understand and ultimately overcome problems with the magnetic field map.

References

[1] CMS Collaboration, *"CMS Physics Technical Design Report"*, CERN/LHCC 2006-001 (2006)

[2] W.-M. Yao et al., Journal of Physics **G33** 1 (2006)

[3] See, for example, the presentation by Sara Bolognesi in the *Muon Barrel Workshop*, April 21-22, 2009; `http://indico.cern.ch/conferenceDisplay.py?confId=56281`